Analyses of Quasielastic and Quasi-Inelastic (^{3}He, t) Scattering from the Ni Isotopes*

P. D. KUNZ, E. ROST, R. R. JOHNSON,† G. D. JONES,‡ AND S. I. HAYAKAWA
Department of Physics and Astrophysics, University of Colorado, Boulder, Colorado 80302

(Received 25 March 1969)

Differential cross sections for 37.5-MeV (^{3}He, t) data have been measured for the Ni isotopes. The data are analyzed using a coupled-channels formalism with both macroscopic and microscopic models for the interaction. The distorted-wave Born approximation, however, is found to be a reasonable approximation. The quasielastic scattering (i.e., excitation of the state in Cu which is the analog of the Ni target ground state) is adequately explained by either model and yields the expected $N-Z$ isotopic dependence. A macroscopic description of the quasi-inelastic scattering (i.e., excitation of the 2^+ analog state) requires a large charge-exchange deformation parameter, in disagreement with results obtained at lower energies for ^{48}Ti. A microscopic description, on the other hand, yields an extracted well depth which is roughly the same for quasielastic and quasi-inelastic scattering. The relative amounts of f and p configuration in the neutron excess are estimated using the microscopic model and are found to be consistent with shell-model calculations.

I. INTRODUCTION

THE study of isobaric analog states by charge-exchange reactions has been valuable in providing information about the symmetry term in the optical potential. A more detailed "microscopic" analysis can also yield additional information about effective nucleon-nucleon interactions and nuclear structure, but requires rather accurate and complete data.

Early studies[1,2] using the (p, n) reaction were limited by energy to the lowest analog state, viz., the "quasielastic" or isobaric ground state (IGS). However, higher states were seen[3] and studied both at low energies[2,4] (where the reaction mechanism is unclear) and at high energies[5] (where individual levels are not resolved). Analog states are also easily excited by (^{3}He, t) reactions[6] and comparable information may be obtained with an easier experiment. However, some discrepancies between the (p, n) and (^{3}He, t) data have been reported[7,8] and are not completely understood.

The analog of the first excited state, or isobaric excited state (IES), has been investigated previously with the (^{3}He, t) reaction.[6,9,10] This transition has been called "quasi-inelastic" scattering[11] when described in a generalized collective-model framework. However, the collective-model analysis of the IES data is not nearly as successful as the corresponding analysis of the IGS. In fact, while the ^{48}Ti(^{3}He, t) IES transition is in good agreement[10] with the collective model, other IES transitions[11,12] in this mass region exceed collective-model predictions by an order of magnitude. To our knowledge, no microscopic model analyses of IES transitions have been reported.

In this experiment, the ground-state and first-excited-state analog cross sections were measured for ^{58,60,62,64}Ni(^{3}He, t) reactions using 37.5-MeV incident ^{3}He ions. In addition, the IGS transition was measured for a ^{61}Ni target in order to study the $N-Z$ dependence of the cross sections. The experiment was designed to obtain IGS and IES data of comparable quality with accurate relative normalizations. The IGS and IES data were then analyzed together using both macroscopic and microscopic descriptions of the charge-exchange interaction process.

The experimental method is described in Sec. II and the data are presented. A brief outline of the theoretical framework is presented and is confronted with the data in Sec. III. Finally, some tentative conclusions are drawn and possibilities for further study are explored.

II. EXPERIMENTAL METHOD

A 37.5-MeV beam of ^{3}He ions was extracted from the University of Colorado Nuclear Physics Laboratory

* Work supported in part by the U.S. Atomic Energy Commission.

† Present address: Department of Physics, University of British Columbia, Vancouver, B. C., Canada.

‡ Present address: Chadwick Laboratory, University of Liverpool, Liverpool, England.

[1] J. D. Anderson and C. Wong, Phys. Rev. Letters **7**, 250 (1961); J. D. Anderson, C. Wong, and J. W. McClure, Phys. Rev. **126**, 2170 (1962); **129**, 2718 (1963).

[2] J. D. Anderson, C. Wong, J. W. McClure, and B. D. Walker, Phys. Rev. **136**, B118 (1964).

[3] J. D. Anderson and C. Wong, Phys. Rev. Letters **8**, 442 (1962).

[4] Y. Ishizaki, Y. Saki, H. Yamaguchi, T. Aizawa, Y. Fumiwama, B. Saheki, K. Yuasa, K. Okane, and N. Yoshimura, Institute of Nuclear Studies Report No. INSJ-97, 1966 (unpublished).

[5] C. J. Batty, R. S. Gimore, and G. H. Stafford, Nucl. Phys. **75**, 599 (1966).

[6] A. G. Blair and H. E. Wegner, Phys. Rev. Letters **9**, 168 (1962); R. Sherr, A. G. Blair, and D. D. Armstrong, Phys. Letters **20**, 392 (1966).

[7] C. D. Goodman, J. D. Anderson, and C. Wong, Phys. Rev. **156**, 1249 (1967).

[8] P. G. Roos, C. A. Ludemann, and J. J. Wesolowski, Phys. Letters **24B**, 656 (1967).

[9] R. R. Johnson, S. Hayakawa, G. Jones, P. D. Kunz, and E. Rost, Bull. Am. Phys. Soc. **13**, 632 (1968); L. F. Hansen, M. L. Stelts, and J. J. Wesolowski, *ibid.* **13**, 632 (1968).

[10] J. J. Wesolowski, E. H. Schwarcz, P. G. Roos, and C. A. Ludemann, Phys. Rev. **169**, 878 (1968).

[11] G. R. Satchler, R. M. Drisko, and R. H. Bassel, Phys. Rev. **136**, B637 (1964).

[12] C. Wong, J. D. Anderson, J. W. McClure, and B. Pohl, Phys. Rev. **156**, 1266 (1967).

TABLE I. Optical-model parameters used to fit the elastic scattering of ^{3}He ions from ^{62}Ni. Set I is an average set of parameters taken from the study in Ref. 18. Set II is obtained from a least-squares search to the 30-MeV data shown in Fig. 2. The Coulomb radius was taken to be equal to 1.4 $A^{1/3}$ F.

	V (MeV)	r_0 (F)	a (F)	W (MeV)	W' (MeV)	r_0' (F)	a' (F)
I	170.6	1.143	0.712	18.5	0	1.60	0.829
II	176.6	1.142	0.744	0	105.5	1.178	0.790

1.3-m FFAG cyclotron[13] and focused to a 0.2-cm-diam spot at the center of the 92-cm scattering chamber.[14] The integrated beam current from a Faraday cup placed 120 cm behind the chamber center was recorded in the first channel of an ND160 pulse-height analyzer. The analyzer was also used to collect the triton spectra, eliminating analyzer dead-time corrections.[15]

The targets were self-supporting foils ranging in thickness from 0.4 to 1.0 mg/cm^2, and were isotopically pure. Particle identification was accomplished by using a semiconductor counter telescope consisting of a 200-μ ΔE silicon surface-barrier detector and a 4700-μ E-ΔE lithium-drifted silicon detector, in conjunction with a pulse-multiplier circuit and conventional electronics.[16] The mass spectrum was continuously monitored during the experiments to ensure correct mass gating for the triton energy spectrum. The over-all resolution for the triton energy spectrum was typically 120-keV full width at half-maximum (FWHM). Figure 1 shows two typical spectra chosen to display the 0^+ and 2^+ analogs of the Ni isotopes in Cu. At the energies used in this experiment there was no difficulty in determining the position of these states. The Q values and isotope shifts in Coulomb displacement energy for the IGS in all cases had good agreement with Coulomb energy systematics.[17] The differential cross sections were measured in the angle range 15°–45° with 2.5° steps in the laboratory.

In order to determine optical-potential parameters for the outgoing tritons, an elastic-scattering experiment using 30-MeV ^{3}He ions was performed with even Ni isotopes as targets. This energy was chosen since it approximates the outgoing triton energy in the experiment. The elastic data of ^{62}Ni are presented in Fig. 2

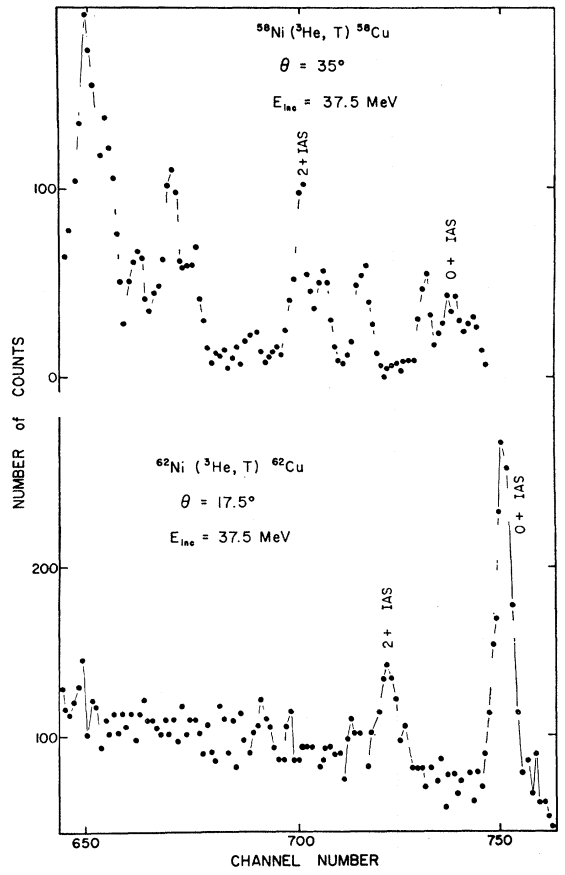

FIG. 1. Triton energy spectra for the Ni(^{3}He, t) reaction at 37.5-MeV incident energy.

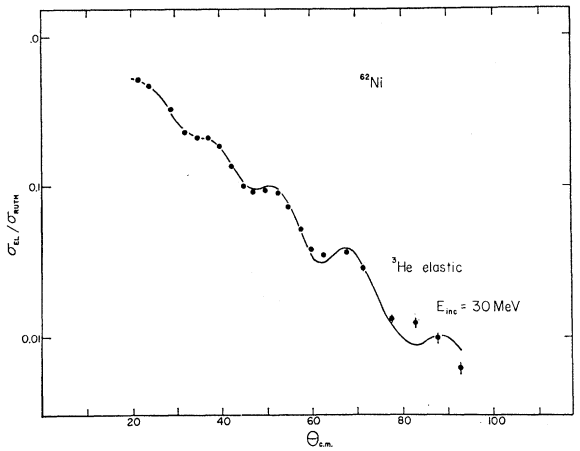

FIG. 2. Elastic scattering ^{3}He data at 30 MeV. The solid line is an optical-model fit using parameter set II given in Table I.

[13] D. A. Lind, J. J. Kraushaar, R. Smythe, and M. E. Rickey, Nucl. Instr. Methods **18,** 62 (1962).
[14] W. S. Gray, R. A. Kenefick, J. J. Kraushaar, and G. R. Satchler, Phys. Rev. **142,** 735 (1966).
[15] P. W. Allison, Rev. Sci. Instr. **35,** 1728 (1964).
[16] G. L. Miller and V. Radeka, Brookhaven National Laboratory Report No. BNL-6952 (unpublished).
[17] R. Sherr, Phys. Letters **24B,** 321 (1967).

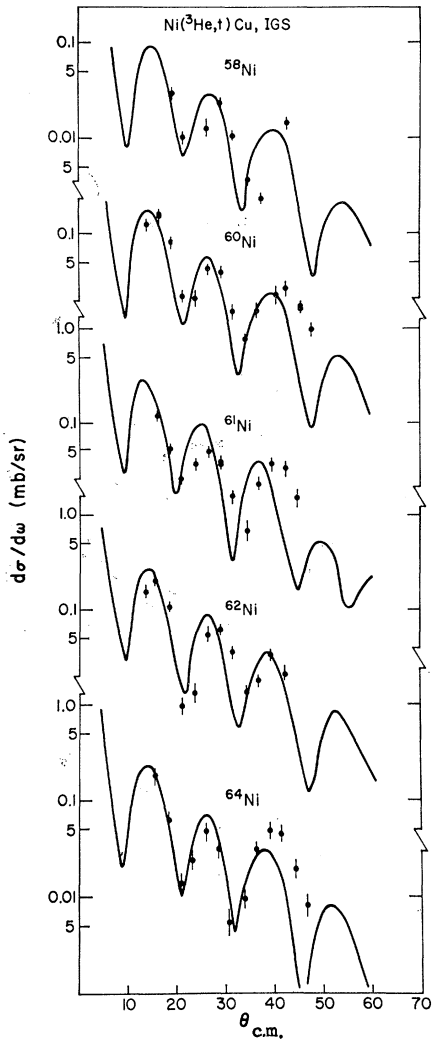

FIG. 3. Triton angular distributions following excitation of the IGS of Cu using the (^{3}He, t) reaction at 37.5 MeV. The solid lines are DWBA curves using a macroscopic model for the interaction.

(which incorporates data from Table I), as is the optical-model fit. The parameters are similar to those found to fit ^{58}Ni elastic data over a wide range of energies.[18] The optical potential used is of the form

$$U(r) = -V(e^x+1)^{-1} - i(W-W'd/dx')(e^{x'}+1)^{-1} + V_c(r), \quad (1)$$

where $x=(r-r_0A^{1/3})/a$, $x'=(r-r_0'A^{1/3})/a'$, and $V_c(r)$ is the Couolmb potential from a uniform sphere of radius $1.4A^{1/3}$ F.

[18] B. W. Ridley, T. W. Conlon, and T. H. Braid, Bull. Am. Phys. Soc. **13,** 117 (1968); E. F. Gibson, B. W. Ridley, J. J. Kraushaar, M. E. Rickey, and R. H. Bassel, Phys. Rev. **155,** 1194 (1967).

The triton parameters are taken to be identical to those measured by the ^{3}He experiment; partial justification of this procedure is given by Wesolowski *et al.*[10] A few calculations were performed using triton parameters extracted from 20-MeV triton elastic data[19] on ^{60}Ni, and also using the prescription of Bassel *et al.*[20] to "correct" the measured ^{3}He parameters. The differences were found to be quite unimportant. The necessary parameters for the incident 37.5-MeV ^{3}He scattering were taken from Gibson *et al.*,[18] and do not differ significantly from the ones determined at 30 MeV.

Figures 3 and 4 give experimental results for angular distributions of tritons following excitation of IGS and IES states of Cu. The solid lines are macroscopic-model distorted-wave Born-approximation (DWBA) curves, to be discussed in Sec. III.

A. Macroscopic Model

To explain the (p, n) reactions on nuclei, Lane[21] has proposed that the optical potentials used to describe the elastic scattering of nucleons be generalized to the form

$$U(r) = U_0(r) + U_1(r)\mathbf{t}\cdot\mathbf{T}/A, \quad (2)$$

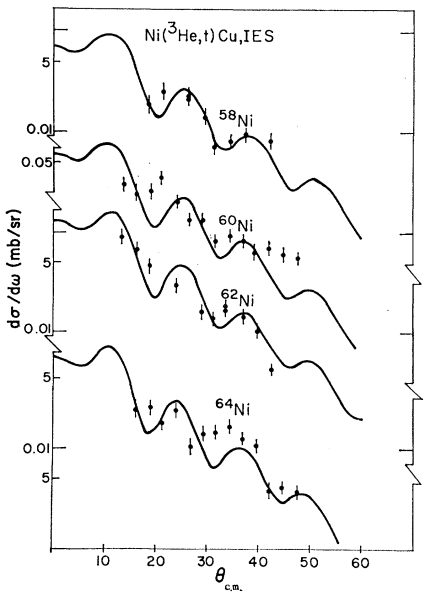

FIG. 4. Triton angular distributions following excitation of the IES of Cu using the (^{3}He, t) reaction at 37.5 MeV. The solid lines are DWBA curves using a macroscopic model for the interaction.

[19] J. C. Hafele, E. R. Flynn, and A. G. Blair, Phys. Rev. **155,** 1238 (1967).

[20] R. H. Bassel, R. M. Drisko, and P. G. Roos, in Proceedings of the International Conference on Nuclear Structure, Tokyo, 1967 (unpublished).

[21] A. M. Lane, Phys. Rev. Letters **8,** 171 (1962); A. Langsford, P. H. Bowen, G. C. Cox, and M. J. N. Saltmarsh, Nucl. Phys. **A113,** 433 (1968).

where $\mathbf{t}$ and $\mathbf{T}$ are the isotopic spin operators for the projectile and nucleus, respectively. The diagonal terms of $\mathbf{t}\cdot\mathbf{T}$ give rise to a symmetry term in the nucleon elastic-scattering potential, while the off-diagonal terms allow for charge-exchange transitions to the isobaric analog ground state. This optical model has been further generalized[11] by deforming both parts of the optical potential, U_0 and U_1. In this manner one has a mechanism to describe the (p, n) reaction to isobaric excited states.

In order to describe the (^{3}He, t) reaction, we assume that the optical potentials for mass-3 particles can be described phenomenologically by a form similar to that for the nucleon potential given in Eq. (2). The set of coupled equations that one derives for the (^{3}He, t) system is then given by[22]

$$[\mathrm{KE}+U_0(\mathrm{He})+2V_c-(2A)^{-1}T_0U_1-E]\Psi(\mathrm{He}) = -A^{-1}(\tfrac{1}{2}T_0)^{1/2}U_1\Psi(t), \quad (3a)$$

$$[\mathrm{KE}+U_0(t)+V_c+\Delta_c+(2A)^{-1}T_0U_1-E]\Psi(t) = -A^{-1}(\tfrac{1}{2}T_0)^{1/2}U_1\Psi(\mathrm{He}). \quad (3b)$$

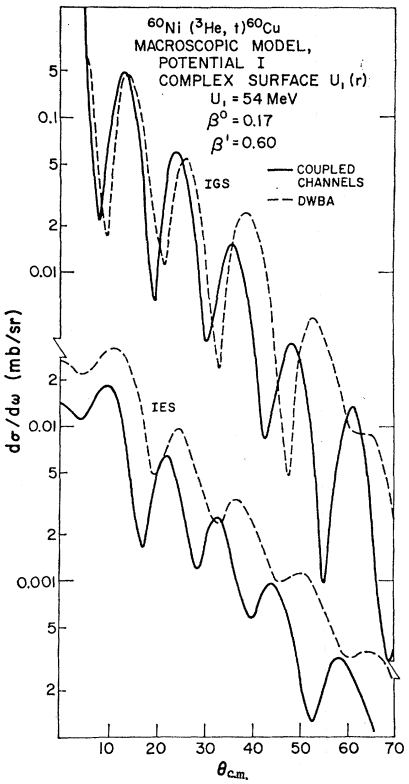

FIG. 5. Comparison of coupled-channel calculations with the DWBA for IGS and IES transitions in the Ni(^{3}He, t) Cu reaction.

[22] G. R. Satchler, in *Isospin on Nuclear Physics*, edited by D. H. Wilkinson (North-Holland Publishing Co., Amsterdam, to be published).

In the above expression, V_c is the Coulomb potential per single electric charge on the projectile, Δ_c is the Coulomb energy difference between the target nucleus and its isobaric analog state, and T_0 is the isotopic spin of the target nucleus. The wave functions $\Psi(\mathrm{He})$ and $\Psi(t)$ are the product function of the scattered particles and nuclear states in the target and analog states, respectively.

In the case of a nucleus with quadrupole deformation, we write the potentials U_0 and U_1 as $U((r-R)/a)$, where the radius R is given by

$$R=R_0(1+\beta Y_{20}(\theta)), \quad (4)$$

where β is a quadrupole deformation parameter, and θ is the angle that the projectile coordinate $\mathbf{r}$ makes with the symmetry axis of the deformed nucleus. Different deformations $\beta^{(0)}$ and $\beta^{(1)}$ are allowed for the U_0 and U_1 terms, respectively. A first-order expansion gives

$$U_i=U_i(x)-\beta^{(i)}(R_i/a_i)\,Y_{20}(\theta)\,(d/dx)\,U_i(x), \quad (5)$$

with $i=0$ or 1, and $x=(r-R_0)/a$. Substitution into Eq. (3) readily yields a system of at most eight coupled equations. The details of the solution to these equations are given elsewhere.[23]

Several calculations were performed using the coupled-channels formalism with "reasonable" parameters to be discussed below. In all cases investigated the DWBA [obtained by treating the right-hand side of (3a) in perturbation, using for $\Psi(t)$ the homogeneous solution of (3b)] was found to be a reasonable approximation. A sample comparison is given in Fig. 5 for the ^{60}Ni(^{3}He, t)^{60}Cu reactions. The coupled channels give a different result than Frahn,[24] who, using a diffraction approximation, predicted an enhancement by a factor of 4 in the quasi-inelastic yield due to non-DWBA terms. Evidently the coherence needed to give this enhancement is not obtained in the coupled-channels method using phenomenological optical potentials and deformation strengths needed to fit the data.[25] The calculations presented in the paper have employed the DWBA for numerical convenience: The only qualitative difference that a coupled-channels analysis would yield is a $\approx$20% reduction in the extracted deformation strengths $\beta^{(1)}$, and a slight shift of the positions of the maxima in the forward angles where the fit to the data is made.

B. Microscopic Model

A less phenomenological approach to the description of inelastic scattering than that given by the collective

[23] T. Tamura, Rev. Mod. Phys. **37**, 679 (1965). The computational work was performed by the coupled-channels code CHUCK on the University of Colorado CDC 6400 computer.

[24] W. E. Frahn, Nucl. Phys. **A107**, 129 (1968).

[25] However, by forcing the adiabatic condition, making the ^{3}He and t distorted waves identical, and using $\beta^{(0)}=\beta^{(1)}$, an effect like that predicted by Frahn was achieved at forward angles.

model uses a more detailed "microscopic" description of the charge-exchange process. This model assumes that the interactions which give rise to the inelastic transitions is a sum of effective two-body forces between the nucleons of the projectile and the nucleons of the target nucleus. We then can write the transition amplitude for a one-step direct process as

$$T_{fi}=\int \chi_f^{(-)*}(\mathbf{r})\,\langle\phi_f\Psi(t)\mid V_{\rm eff}\mid\Psi(\mathrm{He})\phi_i\rangle\chi_i^{(+)}(\mathbf{r})\,d\mathbf{r}. \tag{6}$$

The functions $\chi_i^{(+)}$ and $\chi_f^{(-)}$ are distorted waves describing the initial and final states of relative motion; the intrinsic states of the projectiles and nuclei are denoted by Ψ and ϕ in an obvious notation. The operator $V_{\rm eff}$ is taken to be an effective two-body interaction of the form $V_{\rm eff}=\sum_{kp}t_{kp}$, where k denotes a target nucleon, and p denotes a projectile nucleon. The amplitudes t_{kp} are conveniently parametrized by

$$t_{kp}=(V_{0\alpha}+V_{0\beta}\boldsymbol{\tau}_k\cdot\boldsymbol{\tau}_p+V_{1\alpha}\boldsymbol{\sigma}_k\cdot\boldsymbol{\sigma}_p+V_{1\beta}\boldsymbol{\tau}_k\cdot\boldsymbol{\tau}_p\boldsymbol{\sigma}_k\cdot\boldsymbol{\sigma}_p)\,g(\mid\mathbf{r}_k-\mathbf{r}_p\mid), \tag{7}$$

where $g(r)$ has a Yukawa shape $e^{-\mu r}/\mu r$, and $\boldsymbol{\sigma}$ and $\boldsymbol{\tau}$ are, respectively, twice the spin and isospin operator for the appropriate nucleons. The procedure now is to average the effective interaction $V_{\rm eff}$ over the ^{3}He and triton coordinates. Since the expression one obtains from the three-body projectile averaging gives rather complicated functions,[26] we make the assumption that

$$\langle\Psi(t)\mid V_{\rm eff}\mid\Psi(\mathrm{He})\rangle\approx\sum_k t_k, \tag{8}$$

$$t_k=(V_{0\alpha}'+V_{0\beta}'\boldsymbol{\tau}_k\cdot\boldsymbol{\tau}+V_{1\alpha}'\boldsymbol{\sigma}_k\cdot\boldsymbol{\sigma}+V_{1\beta}'\boldsymbol{\tau}_k\cdot\boldsymbol{\tau}\,\boldsymbol{\sigma}_k\cdot\boldsymbol{\sigma})\,g(\mid\mathbf{r}_k-\mathbf{r}\mid),$$

where the sum is carried over the target nucleons k and the variables $\boldsymbol{\tau}$, $\boldsymbol{\sigma}$, and $\mathbf{r}$ are the isospin, spin, and c.m. coordinates of the projectile, respectively. The strengths V' are suitably modified.[10] This approximation has been discussed by Wesolowski *et al.*[10] in their microscopic description of Ti(^{3}He, t) reactions and seems to be a reasonable one to use.

Since the t_k operators in Eq. (8) are single-particle operators, they connect only nuclear states that differ by at most one nucleon orbit. For the Ni isotopes, we assume the simple shell model where all the levels through the $f_{7/2}$ are filled with both neutrons and protons, and the excess neutrons go into the $p_{3/2}$ and $f_{5/2}$ levels. Thus we write for the $A-56=n$ isotope of Ni and an analog state in the Cu isobar as

$$\begin{aligned}\mid\phi_i\rangle&=\mid(pf)^nI,\ T=\tfrac{1}{2}n,\ M_T=\tfrac{1}{2}n\rangle,\\ \mid\phi_f\rangle&=\mid(pf)^nI',\ T=\tfrac{1}{2}n,\ M_T=\tfrac{1}{2}n-1\rangle.\end{aligned} \tag{9}$$

The isospin part of the matrix element of t_k is easily obtained and yields a factor $\sqrt{n}$ for the $V_{0\beta}$ and $V_{1\beta}$ terms, with the others vanishing. The spatial part is evaluated with a parentage expansion

$$\mid(pf)^nI\rangle=\sum_{\alpha_1J_1}a_{\alpha_1J_1}\mid(pf)^{n-1}\alpha_1J_1\rangle\otimes\mid p_{3/2}\rangle+\sum_{\alpha_2J_2}b_{\alpha_2J_2}\mid(pf)^{n-1}\alpha_2J_2\rangle\otimes\mid f_{5/2}\rangle, \tag{10}$$

where α_1 and α_2 denote additional quantum numbers, and $\otimes$ implies vector coupling to the total angular momentum I.

In this work primary attention is given to the excitation of the IGS in which case $I=I'=0$ and

$$\mid(pf)^n0\rangle=a\mid(pf)^{n-1}\tfrac{3}{2}\rangle\otimes\mid p_{3/2}\rangle+b\mid(pf)^{n-1}\tfrac{5}{2}\rangle\otimes\mid f_{5/2}\rangle,\qquad a^2+b^2=1, \tag{11}$$

holds for target and IGS daughter. By performing a multipole expansion of the interaction

$$g(\mid\mathbf{r}_k-\mathbf{r}\mid)=4\pi\sum_{LM}g_L(r_k,r)\,Y_{LM}(\hat{r}_k)\,Y_{LM}^*(\hat{r}), \tag{12}$$

it is possible to factor the matrix element of $V_{\rm eff}$ into an angular and a radial part. The former is geometrical in nature and is readily dealt with using standard techniques.[27] The radial part is sometimes called a form factor, and for the IGS transition is

$$\begin{aligned}F_0(r)&=a^2\mathcal{g}_p(r)+b^2\mathcal{g}_f(r),\\ \mathcal{g}_l(r)&=\int u_{lj}^{(\pi)}(r_k)\,u_{lj}^{(\nu)}(r_k)\,g_0(r_k,r)\,r_k^2\,dr_k,\end{aligned} \tag{13}$$

where $u_{lj}(r_k)$ are single-particle orbitals for protons π or neutrons ν. Although Eq. (13) may be used as it stands, it is useful to observe that the shape of $\mathcal{g}_l(r)$ at large r is highly independent of l. Thus,

$$F_0(r)\approx(a^2K+b^2)\mathcal{g}_f(r), \tag{14}$$

with $K=\mathcal{g}_p/\mathcal{g}_f$ evaluated at an appropriate large radius. The value of K^2 is conveniently obtained by taking the ratio of cross sections using pure p and pure f orbitals. Although K is slightly dependent on the isotope considered (via the nucleon separation energies), it is rather close to the factor 1.6 for the cases considered here.

With the approximation of Eq. (14), the (^{3}He, t) angular distribution is independent of the parentage coefficients, which appear only as a scale factor $(a^2K+b^2)^2$ in the cross section. This simplicity does not obtain for the IES excitation formula, since the counterpart to Eq. (11) is more involved; in particular, $p\rightarrow f$ transitions are possible, so that terms with ab coefficients appear which *depend on the relative phases* of the parentage expansion. Nevertheless, it is straightforward to

[26] V. A. Madsen, Nucl. Phys. **80**, 177 (1966).

[27] See, e.g., G. R. Satchler, Nucl. Phys. **55**, 1 (1964).

calculate these IES transitions given detailed wave functions, and work along these lines is underway.

The computer code DWUCK was modified to calculate the radial form factors $F_L(r)$ using a Yukawa potential and nuclear wave functions which are solutions to the Schrödinger equation with a Woods-Saxon potential. The calculations were restricted to single orbital transitions (i.e., either $p_{3/2}\rightarrow p_{3/2}$, or $f_{5/2}\rightarrow f_{5/2}$) although we have seen that this is sufficient for IGS transitions. The wave functions for the bound-state nucleons were generated from a Woods-Saxon potential with a radius $1.25A^{1/3}$ F, diffusivity parameter $a=0.65$ F, and a spin-orbit strength 25 times the Thomas term. The proton potential included the potential due to a uniformly charged sphere of radius $1.25A^{1/3}$ F. The depth of the nuclear potential well was adjusted to give the separation energy of each nucleon as tabulated in Table II. The range parameter μ of the Yukawa interaction between projectile and target nucleons was taken

TABLE II. Nucleon separation energies used in the microscopic-model calculations of Ni(^{3}He, t)Cu.

Mass No.	Neutron	Binding energy (MeV) Proton (IGS)	Proton (IES)
58	12.24	2.64	1.24
60	11.39	1.91	0.58
62	10.59	1.24	0.07
64	9.66	0.39	−0.95

to be 1.0 F^{-1}, a value used with success by Satchler and co-workers[14,28] in their (p, p') and (p, n) reaction analyses and by Wesolowski *et al.*[10] in their (^{3}He, t) work. All the calculations to be discussed assume a spin-independent interaction so that the data are fitted with a single strength $V_0\equiv V_{0\beta'}$.

III. RESULTS

A. Dependence on Neutron Excess

The collective-model description of IGS transitions predicts a (^{3}He, t) cross section proportional to the neutron excess, $N-Z$, for an isotopic sequence, as is readily seen in Eq. (3). In the microscopic description, the same dependence occurs if the excess neutrons fill a single orbital throughout the sequence (or if the configuration ratios remain constant). If different orbitals are being filled and contribute unequally to the cross section, a departure from $N-Z$ is to be expected. For IES transitions, the $N-Z$ rule is not expected to hold even with a collective-model description, since there is no *a priori* reason to expect the neutron-excess deformation parameters, $\beta^{(1)}$ in Eq. (5), to be constant for a given isotopic sequence.

TABLE III. Comparison of Ni(^{3}He, t) cross sections with the neutron excess.

Target	$N-Z$	σ_{IGS} [a]	σ_{IES} [b] mb/sr	$\sigma/(N-Z)_{IGS}$	$\sigma/(N-Z)_{IES}$ arbitrary units[c]
^{58}Ni	2	0.23	0.025	1.05	2.5
^{60}Ni	4	0.44	0.020	1.00	1.0
^{61}Ni	5	0.51	...	0.93	...
^{62}Ni	6	0.62	0.040	0.94	1.3
^{64}Ni	8	0.52	0.020	0.59[d]	0.50

[a] Taken at the second peak ($\theta\sim 28°$).
[b] Taken at $\theta=25°$.
[c] Normalized to unity for ^{60}Ni.
[d] An increase to $\sim$0.8 can be obtained if the integrated cross sections are compared or if a DWBA fit is employed (see Table IV).

A comparison of (^{3}He, t) IGS cross sections with the neutron excess is given in Table III, and one sees a rather close proportionality except for ^{64}Ni. A close inspection of Fig. 3 shows that the angular distribution for ^{64}Ni(^{3}He, t) differs from that of the other Ni targets. It is likely that this difference is a ramification of filling

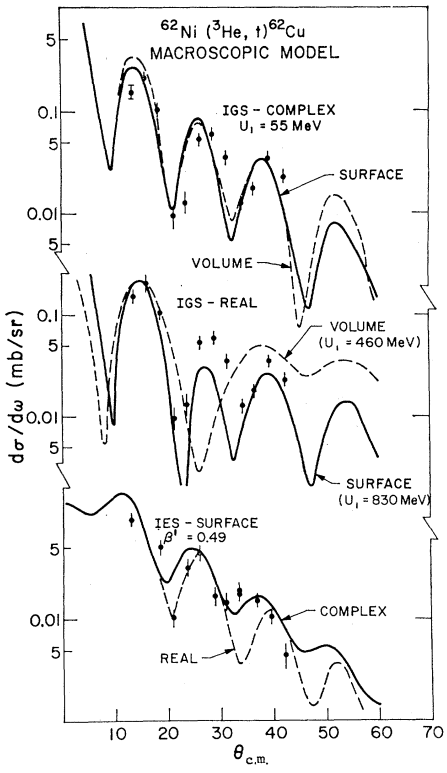

FIG. 6. Study of the effect of geometry choices of the symmetry energy term on the ^{62}Ni(^{3}He, t)^{62} Cu angular distributions (see text). The curves are scaled visually to fit the data as well as possible.

[28] G. R. Satchler, Nucl. Phys. **A95**, 1 (1967).

TABLE IV. Macroscopic-model extraction of symmetry energy parameters from the Ni(^{3}He, t)Cu IGS and IES transitions. A complex surface form of the symmetry energy is assumed. The charge-exchange deformation parameters $\beta^{(1)}$ are defined in Eq. (5).

A	U_1 (MeV)	$\beta^{(1)}$
58	57±3[a]	0.59±0.06[a]
60	54±4	0.41±0.10
61	53±4	...
62	54±3	0.49±0.06
64	49±4	0.34±0.03

[a] Errors reflect only the uncertainty in scaling the DWBA curves to the data.

different neutron orbitals, which is understandable in the microscopic framework. The IES transitions, on the other hand, show no proportionality to $N-Z$ whatever.

B. Macroscopic Model

In order to apply the macroscopic model to the analysis of the (^{3}He, t) data it is necessary to assume a definite geometrical form for the symmetry potential $U_1(r)$. The strength is then obtained by fitting the calculated results to the data. For simplicity, the geometrical parameters needed for U_1 are assumed to be the same as those for U_0, i.e., set I of Table I. For the geometrical shape of $U_1(r)$ we follow the procedure of Bassel *et al.*[20] and take the important imaginary part of $U_1(r)$ to be of surface form, i.e., the derivative of the imaginary part of $U_0(r)$. The less important real part of $U_1(r)$ is taken to be of volume form, viz., proportional to the real part of $U_0(r)$ and is taken to have the same strength as the imaginary part. This procedure (volume real, surface imaginary) is used in the fits in Figs 3 and 4 and is called complex surface in Fig. 6. The sensitivity of the (^{3}He, t) cross sections to the choice of $U_1(r)$ geometry is studied in Fig. 6. A volume choice for the imaginary part (or making it zero) yields a decidedly inferior fit, a fact also noted by Wesolowski *et al.*[10] in their ^{48}Ti(^{3}He, t) study. There is little difference in angular distributions between the real and complex choice for the interaction as long as it is taken to be of surface form. However, the strength of the latter choice is in good agreement with other methods of obtaining the symmetry energy while the real-interaction choice requires a strength an order of magnitude too large. Thus we find a preference for a complex-surface form of the symmetry potential, in agreement with other analyses.[10,20]

The extracted values for U_1 are given in Table IV and are to be compared with the 108-MeV strength obtained by Wesolowski *et al.*[10] in a similar manner for ^{48}Ti, or with the value 35 MeV extracted from elastic-scattering analyses.[20] Here we have multiplied the surface imaginary potential strengths of Wesolowski and Bassel by 4 to agree with our potential definition. In view of the established sensitivity[10] of such results to the ambiguities on the ^{3}He optical parameters, the agreement with other values of the symmetry energy is satisfactory.

The extracted strengths for the IES transitions may be interpreted as neutron-excess deformation parameters, and are seen to be considerably larger than the inelastic deformation parameter $\beta^{(0)}$ ($\beta^{(0)}\approx 0.15$ for the Ni isotopes). A similar result was obtained in early ^{56}Fe(p, n) work, where a value $\beta^{(1)}\approx 0.7$ was extracted. However, in the ^{48}Ti(^{3}He, t) experiment,[10] a value $\beta^{(1)}=0.24$ was obtained, which agreed with the $\beta^{(0)}$ value for ^{48}Ti. Other work is underway to check the later result, and to investigate the correlation between $\beta^{(1)}$ and $\beta^{(0)}$ in this mass region.

Note added in proof. The low IES strength in the ^{48}Ti experiment is indeed correct and may be explained by the exceptional $(f_{7/2})^2$ proton $(f_{7/2})^{-2}$ neutron configuration which results in a broken symmetry for the IES transition. See J. D. McCullen, B. F. Bayman, and Larry Zamick, Phys. Rev. **134,** B515 (1964).

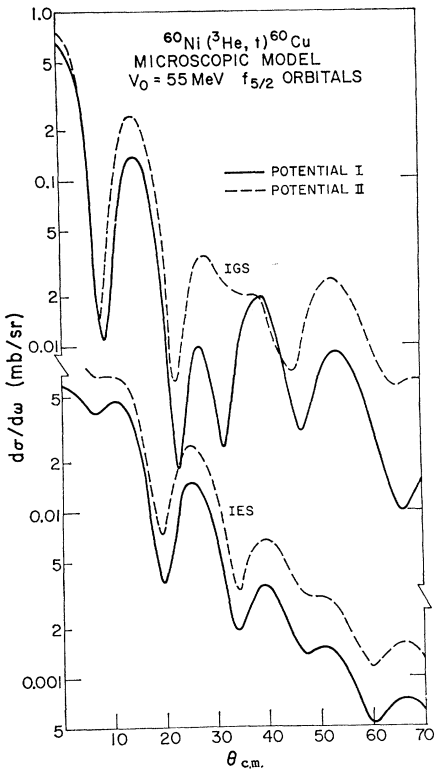

FIG. 7. Microscopic-model fits for ^{60}Ni(^{3}He, t)^{60}Cu IGS and IES transitions using $f_{5/2}$ orbitals. The labels I and II refer to the optical parameters in Table I.

C. Microscopic Model

A microscopic approach to the (^{3}He, t) reaction in terms of nucleon orbitals and a real effective interaction was developed in Sec. II. The resulting cross sections for the ^{60}Ni(^{3}He, t)^{60}Cu IGS and IES transitions are shown in Fig. 7 for both of the optical-parameter choices in Table I assuming $f_{5/2}$ nucleon orbitals. The resulting shapes using $p_{3/2}$ orbitals are essentially identical and differ only in their normalization, the $p_{3/2}$ cross sections being roughly a factor of 2.5 larger as discussed in Sec. II. The normalization strengths needed to fit the data with a pure configuration are given in Table V in terms of V_0, the real two-body interaction strength [denoted as $V_{0\beta}$ in Eq. (8)].

The angular distributions obtained with the microscopic model fit the data ratther badly and are comparable to those obtained using a real, volume symmetry-energy term for the collective model (see Fig. 6). It has been pointed out[28] that the effective interaction may well be complex, and if it were of suitable radial shape could improve the angular distribution. However, the additional parameters involved cannot be determined in this work alone, so we prefer to keep a real interaction.

TABLE V. Microscopic-model extraction of interaction strength parameter V_0 (in MeV) from the Ni(^{3}He, t)Cu IGS and IES transitions. Unmodified optical parameters (set I) are used for the ^{3}He and t scattering.

A	IGS $f_{5/2}$	IGS $p_{3/2}$	IES $f_{5/2}$	IES $p_{3/2}$	IGS mixed[a]
58	54±5[b]	33±3	78±10	48±5	38
60	46±3	30±2	59±3	35±2	33
62	43±4	26±2	56±5	31±3	31
64	40±6	26±3	38±7	22±4	30

[a] Shell-model calculations (see Ref. 29) are used for the relative f-to-p mixing. The b^2/a^2 values are 0.37, 0.58, 0.64, and 0.72 for A = 58, 60, 62, and 64, respectively (see text).

[b] The errors are determined from the range of acceptable normalizations to the data.

Since the maximum at 27° in the 0$^+$ IGS cross section is not reproduced by the theoretical curves, an attempt was made to see what changes in the calculation would improve this fit to this data. In general, any modification to the calculation which would enhance the large-distance behavior of the form factor or distorted waves would increase the size of this almost missing maximum. In particular, the addition of nonlocal effects in the distorted waves or bound-state wave functions as well as a cutoff on the radial integrals would raise this maximum relative to the others. The radial cutoff had the most effect and the calculated cross section for the ^{60}Ni IGS is shown as a function of the lower cutoff in Fig. 8.

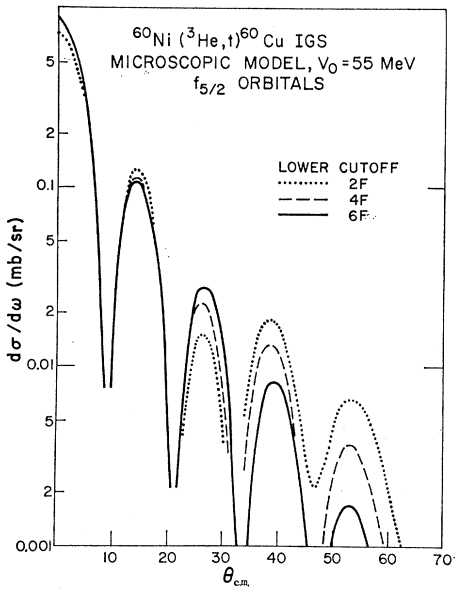

FIG. 8. Sensitivity of ^{60}Ni(^{3}He, t) IGS angular distributions to a lower cutoff on the DWBA radial integrals.

An alternative procedure to improve the fit to the angular distribution is to modify the unmeasured triton optical well. Some change is expected owing to the diagonal-symmetry energy term, and analysis of ^{3}He and t elastic-scattering data at 20 MeV indicate a somewhat smaller (about 2 MeV) real-well depth for the triton and perhaps a smaller imaginary-well radius.[20] Figure 9 shows the effect of these changes on the ^{60}Ni

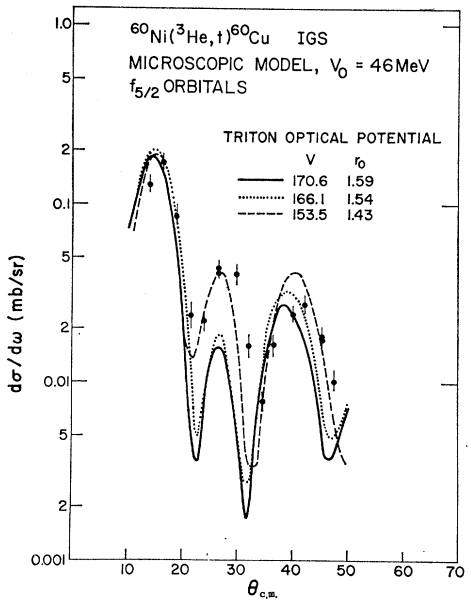

FIG. 9. Sensitivity of ^{60}Ni(^{3}He, t) IGS angular distributions to changes in the triton optical well.

IGS cross section, and it is seen to be unimportant. However, a much larger change in this direction does improve the agreement considerably although the particular combination of triton-well parameters are not well determined. One may also obtain reasonable agreement with a combination of nonlocality and triton-well modification.

In the results presented in Table V, unmodified optical potentials were used with local potentials. Fortunately, the first maximum at 20° is very insensitive to the parameters, and thus the relative strengths may be extracted there with some confidence. Also, the angular distribution of the 2^+ IES is quite insensitive to the calculational details. The values for the effective interaction strengths given in Table V are all in the range $V_0 \approx 50$ MeV for the $f_{5/2} \rightarrow f_{5/2}$ transition and thus compare favorably with the value ~ 55 MeV extracted by Wesolowski *et al.*[10] and the "modified" value of 34 MeV obtained in the $^{52}\mathrm{Cr}(p, n)^{52}\mathrm{Mn}$ analysis.[28]

It is tempting to extend the analysis further and use a shell-model calculation for the parentage coefficients a and b in Eq. (11). The last column in Table V gives V_0 values using b^2/a^2 ratios taken from the work of Cohen *et al.*,[29] who assume an inert ^{56}Ni core, place neutrons in $p_{3/2}$, $f_{5/2}$, $p_{1/2}$, and $g_{9/2}$ orbitals, and solve using an effective "best-fit" two-body interaction. We have summed their $p_{3/2}$ and $p_{1/2}$ configurations in extracting the b^2/a^2 values given in Table V. An appreciable reduction in the spread of V_0 through the Ni isotopes is seen. Part of the remaining variation may be due to assuming a closed $Z=28$ shell. Relaxing this assumption would allow $f_{7/2}$ nucleons to participate in the charge-exchange process. Such core polarization should be more important for the heavier isotopes and would reduce the V_0 spread.

[29] S. Cohen, R. D. Lawson, M. H. Macfarlane, S. P. Pandya, and M. Soga, Phys. Rev. **160,** 903 (1967).

It is not feasible to perform a similar analysis on the IES strengths, since the data are considerably more inaccurate. Also, the parentage coefficients enter sensitively in the radial form factor, and thus it is necessary to test detailed calculations specialized to the analysis. Of course, the sensitivity allows for the possible determination of relative phase information. The pure-configuration IES values of V_0 given in Table V are quite reasonable when compared with the IGS values, the greater spread probably reflecting coherent effects.

IV. CONCLUSIONS

The excitation of analogs to the ground 0^+ state (IGS) and excited 2^+ states (IES) of the Ni isotopes by the (^{3}He, t) reaction may be analyzed using either a macroscopic or microscopic theoretical framework. Good agreement to the angular distributions are obtained for the macroscopic model using a complex symmetry-energy term, the imaginary part of which peaks near the nuclear surface. The IGS transitions are roughly proportional to the neutron excess as expected from a macroscopic model; however, the neutron-excess deformation parameters needed to fit the IES data are larger than the usual quadrupole deformation parameters.

The microscopic-model analysis with a real interaction gives rather poor fits to the angular distribution; however, this can be remedied in several ways. The analysis of the relative cross sections for IGS transitions is consistent with shell-model calculations of the neutron configurations. The strength $V_0 \approx 35$ MeV is in excellent agreement with (p, n) work. A microscopic analysis of the IES transitions in terms of pure orbitals gives reasonable V_0 values. The sensitivity of the IES cross sections to the details of the nucleon orbitals suggests promise for a more elaborate analysis.